SSJ PUBLICATIONS

Journal of Integrated Human Health Sciences

ISSN-3143-8814

Research Article

When Less of the Image is Visible Operational Image Accessibility, Prediction Entropy, and Diagnostic Reconstruction in Breast Ultrasound a Proof-of-Concept Analysis Using BreastMNIST-64

Ahed J Alkhatib[1*]

[1]*Department of Legal Medicine, Toxicology and Forensic Medicine, Jordan University of Science & Technology, Jordan*

***Correspondence:** Alkhatib A.J, Department of Legal Medicine, Toxicology and Forensic Medicine, Jordan University of Science & Technology, Jordan; E-mail: ajalkhatib@just.edu.jo

Received date: 03 Mar 2026: **Accepted date:** 20 Mar 2026: **Published date:** 27 Mar 2026

Copyright: © 2025 Alkhatib A.J. This article is licensed under a Creative Commons Attribution 4.0 International License (CC BY 4.0), which permits use, sharing, adaptation, distribution, and reproduction in any medium or format, provided the original author(s) and source are properly credited.

Abstract

Background: Medical images define a protocol-dependent informational boundary around a biological substrate, but the relations between accessible image content and diagnostic information are rarely formalized.

Objectives: To assess how progressive restriction of the visible image field transforms breast-ultrasound classification, model uncertainty, and case reconstructions of diagnostic likelihood.

Methods: Using the BreastMNIST-64 dataset, we partitioned 780 grayscale breast-ultrasound images into standard training (n=546), validation (n=78), and test (n=156) sets, recoding malignancy as the positive class. Within nested central access domains, we retained 25%, 50%, 75%, or 100% of the image area. We trained a HOG-based standardized logistic regression classifier as the primary transparent model, tuning a single regularization parameter (C=0.01) on the full-image validation set Brier score, then holding it constant across accessibility conditions. Test-set performance was evaluated using the AUC, accuracy, sensitivity, specificity, Brier score, and binary prediction entropy estimated from 1,200 stratified bootstrap samples. A pixel-PCA logistic analysis provided a sensitivity model.

Results: The AUC and accuracy for the primary model were 0.752 [0.619, 0.865], 70.5% [63.9, 76.6] % for 25% access versus 0.775 [0.638, 0.894], 75.0% [69.2, 80.9] % at 50%; 0.832 [0.713, 0.938], 77.6% [72.6, 82.5] % at 75%; and 0.816 [0.674, 0.934], 79.5% [73.9, 85.0] % at 100% access. Prediction entropy declined from 0.692 to 0.532 bits, a reduction of 0.159 bits (95% CI 0.105 to 0.210) across access conditions. Discrimination was not strictly monotonic in image access: AUC at 75% access (0.832) exceeded that of the full image (0.816). Across access conditions, 55/156 (35.3%) cases were reclassified. For discordant cases, accuracy increased from 43.6% at 25% access to 69.1% with full access. The pixel-PCA sensitivity analysis demonstrated a monotonic AUC increase from 0.750 to 0.831.

Conclusions: The diagnostic information within an image is non-linear in the accessible area and depends on the representation. Expanding the visible field generally decreased model uncertainty and improved classification

Citation: Alkhatib A.J (2026). "When Less of the Image is Visible Operational Image Accessibility, Prediction Entropy, and Diagnostic Reconstruction in Breast Ultrasound a Proof-of-Concept Analysis Using BreastMNIST-64" *Journal of Integrated Human Health Sciences, 2*(1):1-12.

SSJ PUBLICATIONS
Journal of Integrated Human Health Sciences
ISSN-3143-8814
Research Article

accuracy but was not strictly monotonic. Our results demonstrate a separation between the biological substrate and diagnostic reconstruction.

Keywords: Breast ultrasound, BreastMNIST, Image accessibility, Diagnostic uncertainty, Prediction entropy, Machine learning, Operational measurement domain

Introduction

Breast ultrasound is widely adopted in diagnostics due to its safety and availability, but its interpretation requires image acquisition quality, operator skill, field of view, lesion location, and information available to the reader or algorithm [1,2]. Artificial intelligence studies have promising results for benign-malignant classification, but recent systematic reviews highlight that internal benchmark accuracy does not equal clinical robustness [3-5].

The Breast Ultrasound Images (BUSI) dataset proposed by Al-Dhabyani et al. [6] comprises normal, benign, and malignant images that can be used to identify breast cancerous tissues. BreastMNIST addresses the same problem but in a lighter version by considering only two classes: a combination of normal and benign categories as one class and malignant category as another. It offers a standardized training, validation, and test partitions for biomedical-image classification tasks [7].

Most image-classification studies ask whether a model can diagnose an image. A different question is how diagnostic reconstruction changes when only part of the image is accessible. This affects cropping, selection of a region of interest, partial image transfer, limited field of view, positioning of the probe, lack of peripheral context information, and other factors by which available information may differ from the full acquired image [8].

Prediction uncertainty offers a different viewpoint. A classifier can improve its confidence without increasing its accuracy, while retaining the possibility for highly confident errors. Reviews in radiology and health care of uncertainty quantification thus advocate distinguishing between discrimination, calibration, quality of probabilities, and uncertainty, rather than treating these as interchangeable notions [9-11].

The design of the present case involves a controlled perturbation of the underlying ultrasound image. Specifically, the central accessible area is expanded while the underlying ultrasound is kept constant. This design does not aim to simulate a clinical ultrasound examination but to investigate if the increase in accessible image content systematically affects diagnostic probabilities, uncertainty, and classification decisions.

The primary hypotheses were that increased accessibility would lead to reduced average prediction uncertainty, improved probability quality and classification performance, and reduced access-dependent disagreement. A secondary hypothesis was that information gain would not necessarily be proportional to visible image area, due to the possible spatial concentration of diagnostically useful content, and model dependency.

Operational Image-Accessibility Framework

For each ultrasound image I, a nested binary mask M_alpha was defined, where alpha represents the visible fraction of total image area.

Citation: Alkhatib A.J (2026). "When Less of the Image is Visible Operational Image Accessibility, Prediction Entropy, and Diagnostic Reconstruction in Breast Ultrasound a Proof-of-Concept Analysis Using BreastMNIST-64" *Journal of Integrated Human Health Sciences, 2*(1):1-12.

SSJ PUBLICATIONS
Journal of Integrated Human Health Sciences
ISSN-3143-8814
Research Article

The accessible image was: I_alpha=M_alpha * I, alpha in {0.25, 0.50, 0.75, 1.00}

The masks were nested central squares. The classifier produced a malignant probability: p_alpha = P(Y = malignant | I_alpha)

Model-dependent binary prediction entropy was: H_alpha=-p_alpha log2(p_alpha) - (1-p_alpha) log2(1-p_alpha) [12]

For expansion from alpha to beta, prediction-entropy reduction was: G (alpha -> beta) = H_alpha - H_beta

Positive G indicates a more concentrated model probability after expansion. Neither thermodynamic entropy nor mutual information. Cross-access reconstruction discordance was defined in the case 0.50-threshold classification was not identical for all four access levels.

Materials and Methods

Dataset

The uploaded BreastMNIST-64 archive contains training, validation, and test images with binary labels. Thus, there were 780 64 × 64 grayscale ultrasound images in the sample. The given labels encode malignant cases as 0 and normal/benign cases as 1; malignancy was converted to the positive class for the current analysis.

There were 546, 78, and 156 images in the training, validation, and test sets, respectively. The latter ones included 42 malignant and 114 normal/benign cases. BreastMNIST is based on BUSI containing the whole set of images, and it simplifies the three-class original BUSI dataset to a binary one [6,7] (Table 1, Figure 1).

Characteristic	Value
Total images	780
Training split	546 (147 malignant; 399 normal/benign)
Validation split	78 (21 malignant; 57 normal/benign)
Test split	156 (42 malignant; 114 normal/benign)
Image format	Grayscale ultrasound, 64 x 64 pixels
Primary task	Malignant vs normal/benign
Primary model	HOG + standardized logistic regression
Sensitivity model	Raw pixels + PCA (95% variance) + logistic regression
Operational access	Central 25%, 50%, 75%, 100% of image area
Bootstrap	1,200 stratified resamples

Table 1. Dataset structure and experimental design

Citation: Alkhatib A.J (2026). "When Less of the Image is Visible Operational Image Accessibility, Prediction Entropy, and Diagnostic Reconstruction in Breast Ultrasound a Proof-of-Concept Analysis Using BreastMNIST-64" *Journal of Integrated Human Health Sciences, 2*(1):1-12.

SSJ PUBLICATIONS
Journal of Integrated Human Health Sciences
ISSN-3143-8814
Research Article

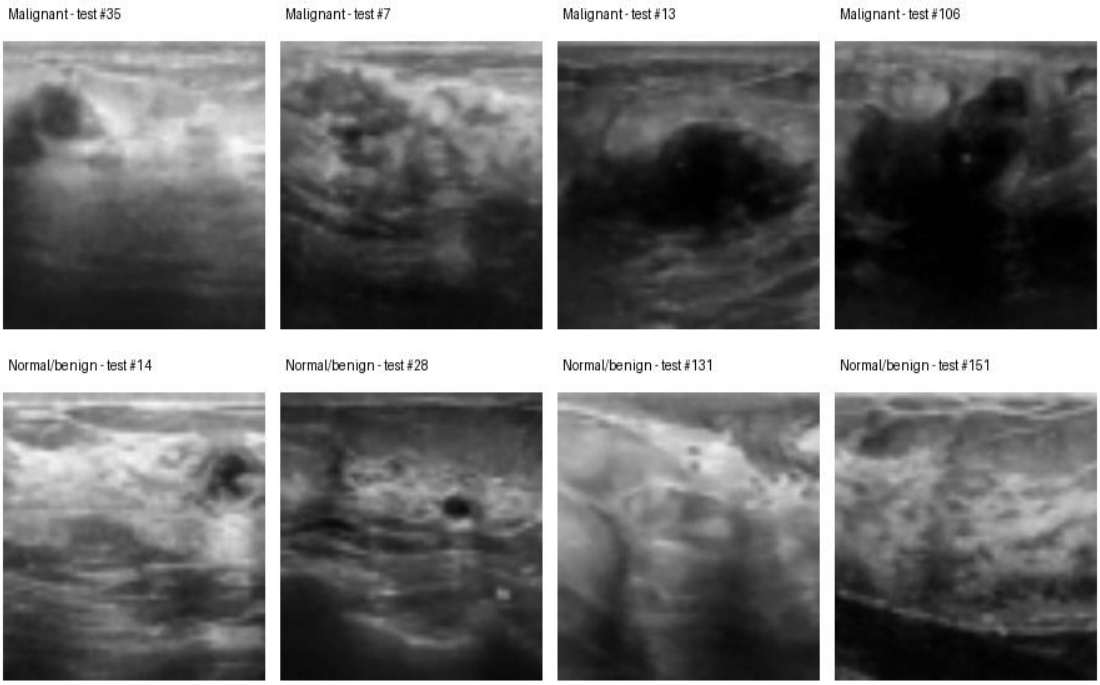


Figure 1. Representative ultrasound images taken directly from the BreastMNIST-64 test data. Images were enlarged only for display and are not generated illustrations

Nested accessibility domains

A centered square showing approx. 25%, 50%, 75%, or 100% of image area was kept, while pixels outside of the accessible square were set to 0. The same transformation was applied to the training, validation, and test images. A separate model was trained under each condition, so that the information available within each domain was tested, rather than a distribution shift in a single full-image model (Figure 2).

Citation: Alkhatib A.J (2026). "When Less of the Image is Visible Operational Image Accessibility, Prediction Entropy, and Diagnostic Reconstruction in Breast Ultrasound a Proof-of-Concept Analysis Using BreastMNIST-64" *Journal of Integrated Human Health Sciences, 2*(1):1-12.

SSJ PUBLICATIONS
Journal of Integrated Human Health Sciences
ISSN-3143-8814
Research Article

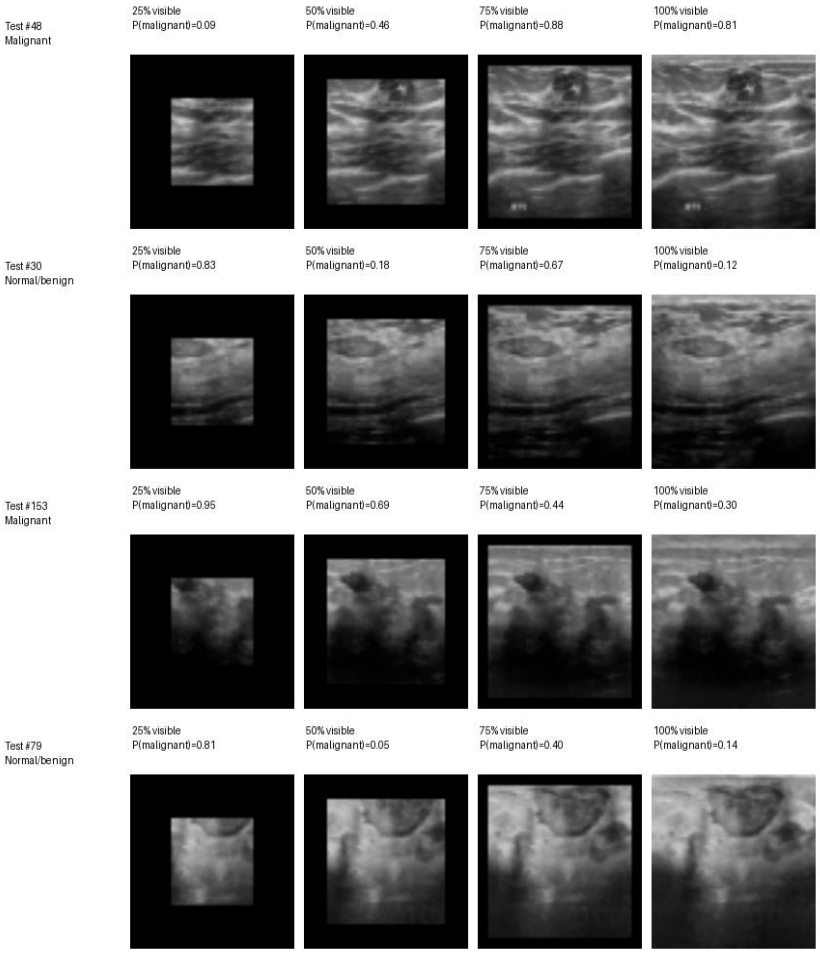


Figure 2. Operational image-accessibility ladder using actual BreastMNIST test images. Each row shows the same ultrasound image under progressively larger accessible central domains. Probabilities are out-of-sample malignant probabilities from the primary model

Primary model

HOG used nine orientations, 8 × 8 pixel cells and 2 × 2 cell blocks [13]. Features were standardized and put into L2 regularized logistic regression with class balanced. Candidate C values were 0.001, 0.01, 0.1, 1 and 10. C=0.01 had the lowest Brier score [14] on the unmasked validation set, and was then fixed for all accessibility conditions. After this one selection step, training and validation data were pooled and condition specific models fitted; the test set was not used for tuning.

Sensitivity model

A second representation squashed to standard pixel vectors masked images retained 95% of variance by principal component analysis [15] and logistic regression with the same C. This tested if the broad access-performance relationship is specific to HOG.

Citation: Alkhatib A.J (2026). "When Less of the Image is Visible Operational Image Accessibility, Prediction Entropy, and Diagnostic Reconstruction in Breast Ultrasound a Proof-of-Concept Analysis Using BreastMNIST-64" *Journal of Integrated Human Health Sciences, 2*(1):1-12.

SSJ PUBLICATIONS
Journal of Integrated Human Health Sciences
ISSN-3143-8814
Research Article

Statistical analysis

The test results were area under the curve (AUC), accuracy at a 0.50 malignant-probability threshold, sensitivity, specificity, Brier score, log loss, and mean binary prediction entropy. We calculated 95% confidence intervals using stratified bootstrap resampling with 1,200 replicates. Paired bootstrap distributions were used to estimate increases in AUC, entropy, and Brier score between nested access domains. An exact McNemar test was used to compare 25% and 100% binary classifications [16]. The analyses were exploratory, because of the small size of the benchmark test set.

Results

Performance by accessible image area

At 25% of accessibility, the primary model demonstrated an AUC of 0.752 and an accuracy of 70.5%. Meanwhile, the AUC rose to 0.775 at 50% of accessibility and 0.832 at 75%. Finally, full-image revealed an AUC of 0.816 and the best accuracy of 79.5%. In general, the overall performance of the model positively correlated with the amount of accessible data; however, it was not strictly monotonic for AUC (Table 2, Figure 3).

Accessible area	AUC (95% CI)	Accuracy	Sensitivity	Specificity	Brier	Entropy
25%	0.752 (0.659-0.835)	70.5%	61.9%	73.7%	0.194	0.692
50%	0.775 (0.692-0.846)	75.0%	57.1%	81.6%	0.176	0.607
75%	0.832 (0.757-0.902)	77.6%	66.7%	81.6%	0.155	0.560
100%	0.816 (0.733-0.891)	79.5%	61.9%	86.0%	0.158	0.532

Table 2. Primary HOG-logistic test performance by accessible image area

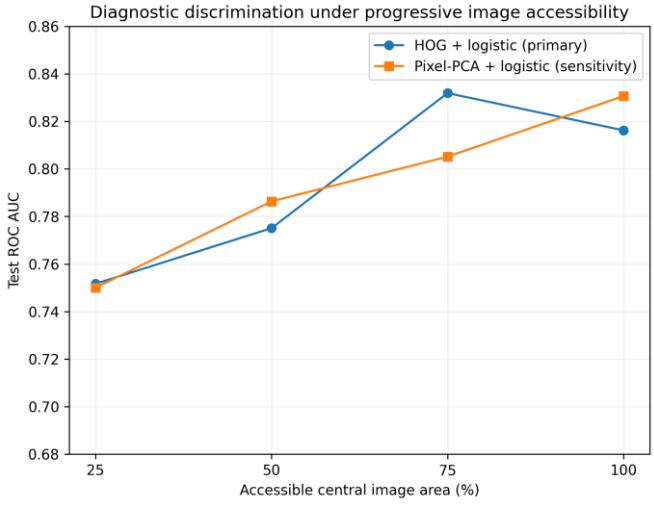


Figure 3. Test AUC across progressive image-access domains. The primary HOG-logistic model and the independent pixel-PCA sensitivity model both improved overall as accessibility expanded, although the primary curve was not strictly monotonic.

Citation: Alkhatib A.J (2026). "When Less of the Image is Visible Operational Image Accessibility, Prediction Entropy, and Diagnostic Reconstruction in Breast Ultrasound a Proof-of-Concept Analysis Using BreastMNIST-64" *Journal of Integrated Human Health Sciences, 2*(1):1-12.

SSJ PUBLICATIONS
Journal of Integrated Human Health Sciences
ISSN-3143-8814
Research Article

Prediction uncertainty

Mean prediction entropy decreased from 0.692 bits at 25% accessibility to 0.607, 0.560, and 0.532 bits at 50%, 75%, and 100%, respectively. The 25%-to-100% expansion decreased entropy by 0.159 bits on average (95% CI 0.105 to 0.210) (Figure 4).

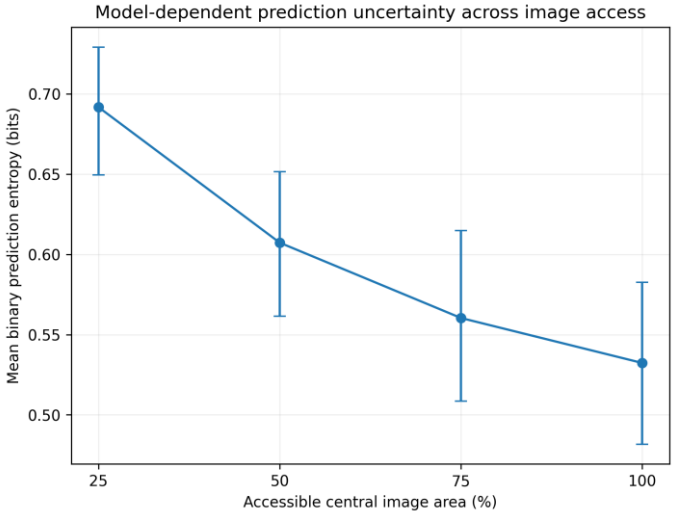


Figure 4. Mean binary prediction entropy across image-access levels. Error bars are stratified bootstrap 95% confidence intervals.

Incremental changes were not proportional to added visible area

The biggest jump in AUC was between 50% and 75% accessibility. Increasing it from 75% to a full image decreased AUC, but further reduced average prediction entropy. Therefore, larger accessible area appeared to consistently boost the probability concentration better than its ranking discriminatory power (Table 3).

From	To	Delta AUC (95% CI)	Entropy reduction (95% CI), bits	Brier improvement (95% CI)	Cases with lower entropy
25%	50%	+0.023 (-0.065 to +0.110)	0.084 (0.036 to 0.133)	+0.019 (-0.017 to +0.056)	60.3%
50%	75%	+0.057 (-0.018 to +0.129)	0.047 (-0.002 to 0.094)	+0.021 (-0.013 to +0.054)	58.3%
75%	100%	-0.016 (-0.063 to +0.028)	0.028 (-0.008 to 0.065)	-0.002 (-0.029 to +0.023)	54.5%
25%	100%	+0.065 (-0.020 to +0.151)	0.159 (0.105 to 0.210)	+0.037 (+0.001 to +0.073)	67.9%

Table 3. Paired changes as the accessible image domain expands

Access-sensitive cases

Classifications were different across access conditions for 55/156 images (35.3%). For cases where classification was correct on at least one access condition, accuracy was better for more access (43.6% for 25% access vs. 69.1% for full access). Classifications for the 101 access-consensus cases were 85.1% accurate. Of the 22 cases that were correct between 25% and 100% access, 8 became correct and 8 became incorrect (exact McNemar p=0.016) (Table 4, Figure 5 and 6).

Citation: Alkhatib A.J (2026). "When Less of the Image is Visible Operational Image Accessibility, Prediction Entropy, and Diagnostic Reconstruction in Breast Ultrasound a Proof-of-Concept Analysis Using BreastMNIST-64" *Journal of Integrated Human Health Sciences, 2*(1):1-12.

SSJ PUBLICATIONS
Journal of Integrated Human Health Sciences
ISSN-3143-8814
Research Article

Accessible area	Correct among discordant	Discordant N	Accuracy among discordant
25%	24	55	43.6%
50%	31	55	56.4%
75%	35	55	63.6%
100%	38	55	69.1%

Table 4. Performance among cross-access discordant test cases

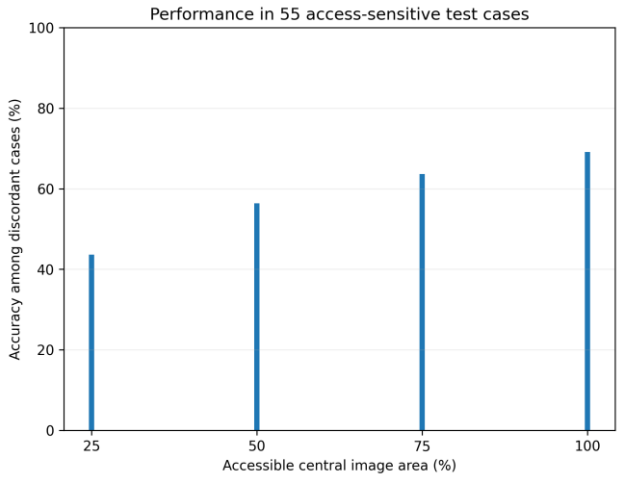


Figure 5. Accuracy within the subset of test cases whose classification changed across accessibility levels

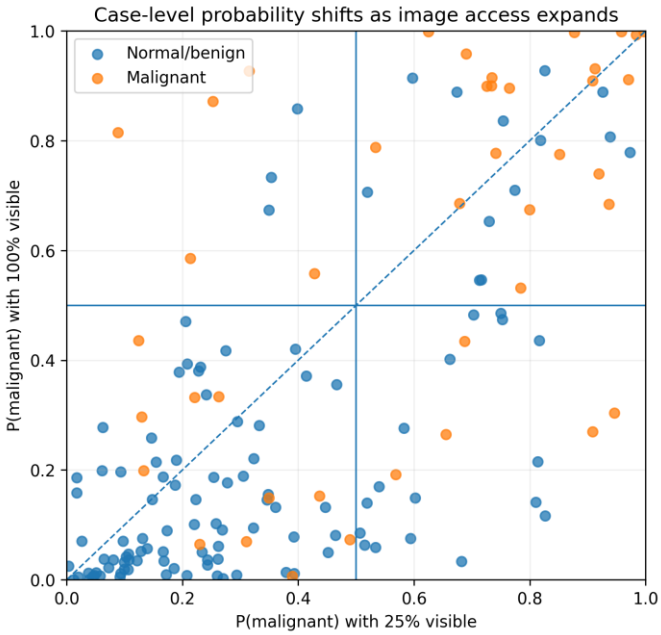


Figure 6. Paired malignant probabilities at 25% and 100% accessibility. Crossing the 0.50 horizontal or vertical threshold indicates access-dependent classification change.

Citation: Alkhatib A.J (2026). "When Less of the Image is Visible Operational Image Accessibility, Prediction Entropy, and Diagnostic Reconstruction in Breast Ultrasound a Proof-of-Concept Analysis Using BreastMNIST-64" *Journal of Integrated Human Health Sciences, 2*(1):1-12.

SSJ PUBLICATIONS
Journal of Integrated Human Health Sciences
ISSN-3143-8814
Research Article

Sensitivity analysis

The independent pixel-PCA model demonstrates a strictly monotonic increase of AUC from 0.750 at 25% to 0.831 at full access. The Brier score and entropy were approximately parallel, supporting the general phenomenon that access to the full image is beneficial, but the specific nature of that benefit depends on the image representation (Table 5).

Accessible area	AUC	Accuracy	Brier	Entropy
25%	0.750	68.6%	0.191	0.774
50%	0.786	73.7%	0.174	0.707
75%	0.805	75.0%	0.170	0.640
100%	0.831	76.9%	0.157	0.580

Table 5. Pixel-PCA-logistic sensitivity analysis

Discussion

This study's proof-of-concept finding demonstrate that diagnostic reconstruction from breast ultrasound is informed by the image domain made accessible to the model. Narrowing the central field reduced discrimination, accuracy, and probability quality; opening it reduced mean prediction entropy; and over a third of test images changed binary classification across the four operational domains. It is the study's central finding that more pixels do not necessarily carry more diagnostic information, as diagnostic information was neither proportional to increased visible area nor universally beneficial to downstream tasks. In the primary model, 75% accessibility achieved a slightly higher AUC than the full image, while achieving lower entropy and higher accuracy with full access. The pixel-PCA sensitivity analysis demonstrated monotonic improvement. Thus, the informational value of newly accessible image content is informed by both the content and the representation.

Recent breast-ultrasound AI literature demonstrates that input design is similarly informative. A 2026 patient-leakage-aware benchmark demonstrated that region-of-interest input could sometimes improve external performance on some cross-dataset settings compared to whole-image input [8]. This experiment is distinct and much simplified, but both findings suggest that larger fields of view do not necessarily encode more usable diagnostic information. Prediction entropy should always be interpreted with caution; as confident wrong models can have low entropy. For that reason, uncertainty was evaluated alongside AUC, Brier score, and classification errors. Contemporary reviews emphasize that uncertainty and confidence measures are useful only when evaluated in conjunction with calibration and predictive validity [9,10,17,18].

The 55 discordant images are of particular interest for future work. These images represent a reconstruction-informed diagnostic state: the same underlying image produces different diagnostic outputs as the accessible context changes. Future work could use the framework to evaluate lesion masks, radiologist-defined regions, saliency analysis, or perilesional tissue bands, to determine whether instability reflects underlying clinically relevant morphology, artifacts, or model-specific dependencies.

The experiment offers an empirical biomedical translation of an operative reconstruction principle. The biological lesion does not change, but the accessible representation does. The reconstructed diagnostic state is therefore

Citation: Alkhatib A.J (2026). "When Less of the Image is Visible Operational Image Accessibility, Prediction Entropy, and Diagnostic Reconstruction in Breast Ultrasound a Proof-of-Concept Analysis Using BreastMNIST-64" *Journal of Integrated Human Health Sciences, 2*(1):1-12.

conditional on what the measurement protocol can observe. This is a finding about inference: observation does not create disease.

The study used transparent classifiers rather than a high-capacity neural network, as BreastMNIST was designed to be a lightweight benchmark and has been evaluated using ResNet and AutoML approaches [7]. The objective was controlled perturbation and interpretability, not benchmark optimization [19].

For clinical translation, the framework should be evaluated on original-resolution images with lesion boundaries, scanner metadata, and independent cohorts [1,2,20]. Recent reviews and dataset-shift studies demonstrate that breast-ultrasound AI remains sensitive to study design, acquisition heterogeneity, and external validation [3,8]. TRIPOD+AI and PROBAST+AI both emphasize transparent reporting and independent evaluation [21,22].

Proposed Operational Principles for Biomedical Imaging

The results support three cautious, testable propositions:

1. **Accessibility dependence**: diagnostic probability depends on the image representation made accessible.

$$P(Y \mid I_{alpha}) \text{ need not equal } P(Y \mid I_{beta})$$

2. **Access quantity is not information quantity**: a larger visible area does not guarantee proportional improvement in discrimination.

$$beta > alpha \text{ does not necessarily imply } AUC_{beta} > AUC_{alpha}$$

3. **Reconstruction stability is case dependent**: some images retain the same classification across access levels, while others are access sensitive.

These propositions concern measurement and inference rather than the biological ontology of cancer.

Limitations

- BreastMNIST-64 only contains 780 low-resolution images and the official test split contains 156 images, leading to widely varying confidence intervals.
- The benchmark collapses normal and benign images into one nonmalignant class and therefore does not reproduce the full clinic differential diagnosis.
- The 64 x 64 images are standardized derivatives rather than original-resolution examinations.
- Central masking is an experimental perturbation and is not a literal simulation of probe field-of-view restriction or lesion-centered acquisition.
- No lesion masks or radiologist-defined regions are included in the uploaded NPZ file, so access domains were geometric rather than anatomy-informed.
- The primary HOG-logistic classifier was intentionally simple and not state of the art.
- Prediction entropy is model dependent and is not a direct measure of biological uncertainty.
- Only internal evaluation on the predefined BreastMNIST test split was possible; external validation is required.
- Detailed patient, scanner, and acquisition metadata were unavailable in the uploaded archive.

Conclusion

Citation: Alkhatib A.J (2026). "When Less of the Image is Visible Operational Image Accessibility, Prediction Entropy, and Diagnostic Reconstruction in Breast Ultrasound a Proof-of-Concept Analysis Using BreastMNIST-64" *Journal of Integrated Human Health Sciences, 2*(1):1-12.

SSJ PUBLICATIONS
Journal of Integrated Human Health Sciences
ISSN-3143-8814
Research Article

Progressively increasing the accessible image domain consistently increased diagnostic reconstruction accuracy while decreasing model-dependently predicted entropy in BreastMNIST-64. However, diagnostic information is not linearly related to visible image area, since the primary model achieved its highest AUC at 75% access while lowest entropy and highest accuracy were attained with the complete image. Additionally, over one-third of test images changed classification results across access conditions. These findings warrant establishing a formal distinction between the biological lesion, the accessible image representation and reconstructed diagnostic state. The strongest next test would involve an original-resolution breast-ultrasound dataset with lesion masks, permits comparing lesion core, margin, perilesional tissue, and surrounding parenchyma as biologically meaningful operational domains.

Data Availability

The study used the BreastMNIST-64 NPZ dataset supplied for this analysis. BreastMNIST is part of MedMNIST and is derived from the public BUSI dataset [6,7].

Ethics Statement

This study is a secondary analysis of a publicly distributed, de-identified benchmark dataset and involved no new participant recruitment or intervention.

References

1. Huang, L., Zhou, J., Jiao, J., Zhou, S., Chang, C., Wang, Y., & Guo, Y. (2024). Standardization of ultrasound images across various centers: M2O-DiffGAN bridging the gaps among unpaired multi-domain ultrasound images. *Medical Image Analysis*, *95*, 103187.
2. Kelly, C. J., Karthikesalingam, A., Suleyman, M., Corrado, G., & King, D. (2019). Key challenges for delivering clinical impact with artificial intelligence. *BMC medicine*, *17*(1), 195.
3. Dan, Q., Xu, Z., Burrows, H., Bissram, J., Stringer, J. S., & Li, Y. (2024). Diagnostic performance of deep learning in ultrasound diagnosis of breast cancer: a systematic review. *NPJ precision oncology*, *8*(1), 21.
4. Li, H., Zhao, J., & Jiang, Z. (2024). Deep learning-based computer-aided detection of ultrasound in breast cancer diagnosis: A systematic review and meta-analysis. *Clinical Radiology*, *79*(11), e1403-e1413.
5. Liu, J., Pian, L., Chen, J., Zhao, J., Liu, Y., Meng, F., & Zeng, C. (2025). Artificial intelligence in breast ultrasound: a systematic review of research advances. *Frontiers in Oncology*, *15*, 1619364.
6. Al-Dhabyani, W., Gomaa, M., Khaled, H., & Fahmy, A. (2020). Dataset of breast ultrasound images. *Data in brief*, *28*, 104863.
7. Yang, J., Shi, R., Wei, D., Liu, Z., Zhao, L., Ke, B., ... & Ni, B. (2023). Medmnist v2-a large-scale lightweight benchmark for 2d and 3d biomedical image classification. *Scientific data*, *10*(1), 41.
8. Wang, L. (2026). Breast Ultrasound AI Under Dataset Shift: A Patient-Leakage-Aware Benchmark. *Diagnostics*, *16*(10), 1537.
9. Chua, M., Kim, D., Choi, J., Lee, N. G., Deshpande, V., Schwab, J., ... & Do, S. (2023). Tackling prediction uncertainty in machine learning for healthcare. *Nature Biomedical Engineering*, *7*(6), 711-718.
10. Faghani, S., Moassefi, M., Rouzrokh, P., Khosravi, B., Baffour, F. I., Ringler, M. D., & Erickson, B. J. (2023). Quantifying uncertainty in deep learning of radiologic images. *Radiology*, *308*(2), e222217.
11. Seoni, S., Jahmunah, V., Salvi, M., Barua, P. D., Molinari, F., & Acharya, U. R. (2023). Application of uncertainty quantification to artificial intelligence in healthcare: A review of last decade (2013–2023). *Computers in Biology and Medicine*, *165*, 107441.

Citation: Alkhatib A.J (2026). "When Less of the Image is Visible Operational Image Accessibility, Prediction Entropy, and Diagnostic Reconstruction in Breast Ultrasound a Proof-of-Concept Analysis Using BreastMNIST-64" *Journal of Integrated Human Health Sciences, 2*(1):1-12.

SSJ PUBLICATIONS

Journal of Integrated Human Health Sciences

ISSN-3143-8814

Research Article

12. Shannon, C. E. (1948). A mathematical theory of communication. *The Bell system technical journal*, *27*(3), 379-423.
13. Dalal, N., & Triggs, B. (2005, June). Histograms of oriented gradients for human detection. In *2005 IEEE computer society conference on computer vision and pattern recognition (CVPR'05)* (Vol. 1, pp. 886-893). Ieee.
14. Glenn, W. B. (1950). Verification of forecasts expressed in terms of probability. *Monthly weather review*, *78*(1), 1-3.
15. Jolliffe, I. T., & Cadima, J. (2016). Principal component analysis: a review and recent developments. *Philosophical transactions. Series A, Mathematical, physical, and engineering sciences*, *374*(2065), 20150202.
16. McNemar, Q. (1947). Note on the sampling error of the difference between correlated proportions or percentages. *Psychometrika*, *12*(2), 153-157.
17. Guo, C., Pleiss, G., Sun, Y., & Weinberger, K. Q. (2017, July). On calibration of modern neural networks. In *International conference on machine learning* (pp. 1321-1330). PMLR.
18. Van Calster, B., McLernon, D. J., Van Smeden, M., Wynants, L., Steyerberg, E. W., & Topic Group 'Evaluating diagnostic tests and prediction models' of the STRATOS initiative Bossuyt Patrick Collins Gary S. Macaskill Petra McLernon David J. Moons Karel GM Steyerberg Ewout W. Van Calster Ben van Smeden Maarten Vickers Andrew J. (2019). Calibration: the Achilles heel of predictive analytics. *BMC medicine*, *17*(1), 230.
19. Evangelia, C., Jie, M., Collins, G., Steyerberg, E., Verbakel, J., & Van Calster, B. (2019). A systematic review shows no performance benefit of machine learning over logistic regression for clinical prediction models. *Journal of Clinical Epidemiology*, *110*.
20. Luo, L., Wang, X., Lin, Y., Ma, X., Tan, A., Chan, R., ... & Chen, H. (2024). Deep learning in breast cancer imaging: A decade of progress and future directions. *IEEE Reviews in Biomedical Engineering*, *18*, 130-151.
21. Collins, G. S., Moons, K. G., Dhiman, P., Riley, R. D., Beam, A. L., Van Calster, B., ... & Logullo, P. (2024). TRIPOD+ AI statement: updated guidance for reporting clinical prediction models that use regression or machine learning methods. *bmj*, *385*.
22. Moons, K. G., Damen, J. A., Kaul, T., Hooft, L., Navarro, C. A., Dhiman, P., ... & Van Smeden, M. (2025). PROBAST+ AI: an updated quality, risk of bias, and applicability assessment tool for prediction models using regression or artificial intelligence methods. *bmj*, *388*.

Citation: Alkhatib A.J (2026). "When Less of the Image is Visible Operational Image Accessibility, Prediction Entropy, and Diagnostic Reconstruction in Breast Ultrasound a Proof-of-Concept Analysis Using BreastMNIST-64" *Journal of Integrated Human Health Sciences, 2*(1):1-12.